

Silver-Enhanced Imaging of DNA Hybridization at DNA Microarrays with Scanning Electrochemical Microscopy

Jun Wang, Fayi Song, and Feimeng Zhou*

Department of Chemistry and Biochemistry, California State University, Los Angeles,
Los Angeles, California 90032

Received December 18, 2001. In Final Form: April 24, 2002

The use of scanning electrochemical microscopy (SECM) to image oligodeoxynucleotide (ODN) hybridization at spots on microarrays has been demonstrated. ODN probes at a microarray surface were hybridized with a biotinylated target, and the regions where sequence-specific hybridization had occurred were developed by the silver staining process (adsorption of streptavidin–gold nanoparticles followed by silver particle deposition). As a consequence of the staining process, the surface conductivity of the region where hybridization had taken place increased. Such an increase in conductivity was sensitively detected by a SECM tip. The SECM detection level for a 17mer target was found to be at 30 amol per spot (or 3.0 fmol per slide). These values compare well with those from other detection methods (e.g., fluorescence and colorimetric detections). Coupled with the alteration of the hybridization temperature, sequence-specific (single-base mismatch) DNA analysis can be accomplished. A reasonable sample throughput (imaging an area of 0.24 cm × 0.24 cm in about 38 min at a tip scanning speed of 50 μm/s) was obtained.

1. Introduction

There has been a tremendous effort geared toward the fabrication of DNA microarrays and the development of sensitive, selective, and high-throughput DNA microarray chip detectors (readers).¹ The impetus behind such an effort stems from the potential of the DNA chips for applications in disease diagnosis and gene expression.^{1–6} The most popular DNA chip imaging techniques rely on the detection of the duplex formation between probes (on the chip) and targets (in the sample solution) labeled with a fluorescent or radioactive marker.^{1,2} These techniques have been demonstrated to possess a high sample throughput and to be extremely sensitive. However, the detection of fluorophore-tagged targets typically involves the use of a relatively expensive confocal fluorescence scanner and is not applicable to nylon membrane-based microarrays,¹ while labeling targets with radioactive markers exposes the analyst to hazardous materials. Therefore, it is imperative to develop less expensive methods that permit the sensitive detection of hybridization in highly localized regions on a microarray without involving the use of hazardous markers. For example, chemiluminescence, colorimetric detection, and scanometric DNA array detection with nanoparticle-labeled probes have been reported as useful techniques for reading DNA chips.^{1,7–10}

Scanning probe microscopy (SPM) is a versatile and relatively new biophysical technique for DNA analysis and can provide information that is not extractable from other traditional molecular biology methods.^{11–13} For example, atomic force microscopy (AFM) has been shown to be a powerful technique for applications as diverse as measurement of force associated with DNA duplex formation/dissociation,¹⁴ visualization of DNA–protein interactions,¹² and detection of single-base mismatches.¹⁵ The operation of SPM in solutions under physiological conditions is particularly attractive, as the dynamic biological processes can be monitored without greatly perturbing the structures of the surface-confined biomolecules.

Scanning electrochemical microscopy (SECM),^{16,17} a variant of SPM, has become a powerful analytical tool to image biomolecules immobilized onto various surfaces.^{18–29}

* To whom correspondence should be addressed. Phone: 323 343 2390. Fax: 323 343 6490. E-mail: fzhou@calstatela.edu.

(1) Sanchez-Carbayo, M.; Bornmann, W.; Cordon-Cardo, C. *Curr. Org. Chem.* **2000**, *4*, 945–971.

(2) Nelson, T. R. *Chip, Chip, Array! An Analysis of DNA Chip Technology*; Dain Rauscher Wessels: Minneapolis, MN, 2000.

(3) Thorp, H. H. *Trends Biotechnol.* **1998**, *16*, 117–121.

(4) O'Donnell, M. J.; Tang, K.; Koster, H.; Smith, C. L.; Cantor, C. R. *Anal. Chem.* **1997**, *69*, 2438–2443.

(5) Southern, E. M.; Case-Green, S. C.; Elder, S. C.; Johnson, M.; Mir, K. U.; Wang, L.; Williams, J. C. *Nucleic Acids Res.* **1994**, *22*, 1368–1373.

(6) Schena, M.; Shalon, D.; Davis, R. W.; Brown, P. O. *Science* **1995**, *270*, 467–470.

(7) Taton, T. A.; Mirkin, C. A.; Letsinger, R. L. *Science* **2000**, *289*, 1757–1760.

(8) Reynolds, R. A., III.; Mirkin, C. A.; Letsinger, R. L. *J. Am. Chem. Soc.* **2000**, *122*, 3795–3796.

(9) Storhoff, J. J.; Elghariani, R.; Mucic, R. C.; Mirkin, C. A.; Letsinger, R. L. *J. Am. Chem. Soc.* **1998**, *120*, 1959–1964.

(10) Alexandre, I.; Hamels, S.; Dufour, S.; Collet, J.; Zammattio, N.; Longueville, F. D.; Gala, J.-L.; Remacle, J. *Anal. Biochem.* **2001**, *295*, 1–8.

(11) Takano, H.; Kenseth, J. R.; Wong, S.-S.; O'Brien, J. C.; Porter, M. D. *Chem. Rev.* **1999**, *99*, 2845–2890.

(12) Pope, L. H.; Davies, M. C.; Roberts, C. J.; Tendler, S. J. B.; Williams, P. M. *Anal. Commun.* **1998**, *35*, 5H–7H.

(13) Lillehei, P. T.; Bottomley, L. A. *Anal. Chem.* **2000**, *72*, 189–196.

(14) Noy, A.; Vezenov, D. V.; Kayyem, J. F.; Meade, T. J.; Lieber, C. M. *Chem. Biol.* **1997**, *4*, 519–527.

(15) Lioubashevski, O.; Patolsky, F.; Willner, I. *Langmuir* **2001**, *17*, 5134–5136.

(16) Bard, A. J.; Fan, F.-R. F.; Pierce, D. T.; Unwin, P. R.; Wipf, D. O.; Zhou, F. *Science* **1991**, *254*, 68–74.

(17) Bard, A. J.; Fan, F.-R. F.; Mirkin, M. V. *Scanning Electrochemical Microscopy*; Bard, A. J., Ed.; Marcel Dekker: New York, 1994; Vol. 18, pp 244–391.

(18) Fan, F.-R. F.; Bard, A. J. *Proc. Natl. Acad. Sci. U.S.A.* **1999**, *96*, 14222–14227.

(19) Horrocks, B. R.; Schmidtke, D.; Heller, A.; Bard, A. J. *Anal. Chem.* **1993**, *65*, 3605–3614.

(20) Pierce, D. T.; Unwin, P. R.; Bard, A. J. *Anal. Chem.* **1992**, *64*, 1795–1804.

(21) Wijayawardhana, C. A.; Wittstock, G.; Halsall, H. B.; Heineman, W. R. *Electroanalysis* **2000**, *12*, 640–644.

(22) Wijayawardhana, C. A.; Wittstock, G.; Halsall, H. B.; Heineman, W. R. *Anal. Chem.* **2000**, *72*, 333–338.

(23) Wang, J.; Wu, L.-H.; Li, R. *J. Electroanal. Chem.* **1989**, *272*, 285–292.

(24) Nowall, W. B.; Wipf, D. O.; Kuhr, W. G. *Anal. Chem.* **1998**, *70*, 2601–2606.

Studies of enzymatic reactions,^{19–22,25,26} antigen–antibody interactions,^{24,28} and living cells³⁰ have been reported. While the typical SECM resolution does not approach that of AFM and scanning tunneling microscopy (STM) (though a recent report by Fan and Bard has shown that SECM can also be used to image immobilized nucleic acid and protein molecules¹⁸), the technique possesses certain unique features that cannot be rivaled by other SPMs. SECM is capable of imaging chemical or biochemical activities present at a surface and can scan samples whose sizes (e.g., areas as large as a few cm²) are much larger than that generally accessible to AFM or STM. The latter feature makes SECM particularly advantageous over other SPMs for imaging DNA microarrays, since the area of a microarray to be read far exceeds the range that is amenable to AFM or STM. Furthermore, SECM lateral resolution (micrometer or submicrometer)^{16,17} is sufficient for imaging even DNA arrays of relatively high density whose spots are tens of micrometers or greater.^{1,2} Finally, SECM, like most other electrochemical instrumentation, is relatively inexpensive, compact, and sensitive (particularly to the surface conductivity changes and to the detection of products arising from the substrate surface), and its well-developed theory can help interpret the observed surface activities.

Thus far, the potential of SECM for sensitive detection of hybridization events at DNA microarrays has not been fully explored. Takenaka and co-workers recently reported their preliminary studies on the visualization of DNA microarrays by SECM with the aid of an electroactive hybridization indicator.²⁷ While the report demonstrates the feasibility of SECM for reading the microarray surface, the DNA hybridization detection levels were lower than those of other existing analytical techniques. Moreover, the mechanism for the SECM detection was not clear, as whether the SECM tip was in contact with the DNA duplexes on the microarray surface and how the electroactive hybridization indicator provided the SECM feedback current were not elucidated.

We report here our work on the utilization of SECM as a highly sensitive detector of imaging hybridization at localized spots on microarray surfaces. Our approach takes advantage of the superb sensitivity of SECM toward the small variation of conductivities at the substrate surface. The SECM imaging was conducted in conjunction with the development (enhancement) of the spots that had undergone hybridization reactions by the well-known silver staining processes. Several recent reports have shown that the silver staining processes can enhance various DNA detection schemes.^{7,9,10,31,32} The deposition of silver nanoparticles onto locations where sequence-specific hybridization had occurred afforded a much higher SECM feedback current. This methodology possesses a high sensitivity and is capable of detecting single-base mismatches. Our approach should complement other existing methods for sequence-specific DNA analysis (e.g.,

fluorescence or colorimetric detection and scanometric DNA array detection with nanoparticle probes).

2. Experimental Section

Materials. Hexaamineruthenium(III) chloride (Ru(NH₃)₆Cl₃), Tris-HCl, and NaCl were purchased from Aldrich Chemicals. The Silver Blue kit and the hybridization buffer were acquired from Advanced Array Technology (AAT, Belgium). All stock solutions were prepared daily with deionized water. The washing buffer and microspotting solutions were obtained from TeleChem International (Sunnyvale, CA). Oligodeoxynucleotide (ODN) probes with one end modified with aminoethyl or aminoheptyl groups and the target biotinylated at the 5' end were all obtained from Integrated DNA Technologies (Coralville, IA). The four ODN probes have the following sequences:



and the sequence of the biotinylated target is 3'-CATTTTGCT-GCCGGTCA-5'-biotin.

Probe 1 has a sequence complementary to that of the target, probe 2 has a single-base mismatch, probe 3 has three mismatching bases, and probe 4 is noncomplementary to the target. The bases of probes mismatching the target are *underlined*.

Instrumentation. The SECM apparatus was constructed based on the design described in ref 16. A 11- μm -diameter carbon fiber ultramicroelectrode (UME) was employed as the SECM tip. The auxiliary and reference electrodes were a Pt wire and a Ag/AgCl electrode, respectively. The DNA microarray slide was sandwiched between a Teflon cell and a Teflon base plate. This cell assembly was secured onto a tilt platform (Edmund Industrial Optics, Barrington, NJ).

Construction of the DNA Spotting Device. The DNA spotting device was built in house by mounting a SPH32 pinhead (TeleChem International) onto the sampling arm of a HPLC auto-sampler (ISS-100, Perkin-Elmer Corp., Norwalk, CT). Pins with an internal volume of 0.6 μL (model SMP4B, Telechem International) were mounted onto the pinhead, and the probe solutions were contained in vials that situated at the predetermined positions of the auto-sampler. These pins are designed to deliver 1.2 nL of DNA solution per spot and would yield spots of an average diameter of ca. 130–155 μm on a commercial DNA microarrayer (SpotBot, Telechem International).

Procedures. (a) *DNA Microarray Fabrication, DNA Hybridization, and Silver Particle Deposition.* For the microarray fabrication, an aldehyde-modified glass slide (SMA-25, TeleChem International) was first mounted onto an *x-y* translation stage (Thorlabs, Newton, NJ). To place spots of probe solutions, the slide was manually moved in the *x* or *y* direction through adjusting the micrometers on the stage. The DNA probe concentration was 10 μM . Because the mechanical stability of our homemade spotter is not as good as that of a commercial spotting device and it is difficult to control the pressure and time of the contact between the pin and slide, the resultant spots were larger than that potentially achievable with the specific spotting pin. The spots had an average diameter of 300 μm , and the center-to-center distance between spots was typically 500 μm . Despite the relatively large spots and wide separations between adjacent spots, our home-built DNA microarray spotter can produce relatively regular arrays of spots with a circular or oval shape. Arrays were rinsed with a 0.2% sodium dodecyl sulfonate (SDS) solution and water to desorb the nonspecifically adsorbed probes and dried, and the unreacted aldehyde groups were deactivated by treating with a 0.3% sodium borohydride solution for 5 min, followed by rinsing with a SDS solution and water.

(25) Wittstock, G.; Yu, K.-J.; Halsall, H. B.; Ridgeway, T. H.; Heineman, W. R. *1995*, *67*, 3578–3582.

(26) Wittstock, G.; Schuhmann, W. *Anal. Chem.* **1997**, *69*, 5059–5066.

(27) Yamashita, K.; Takagi, M.; Uchida, K.; Kondo, H.; Takenaka, S. *Analyst* **2001**, *126*, 1210–1211.

(28) Shiku, H.; Matsue, T.; Uchida, I. *Anal. Chem.* **1996**, *68*, 1276–1278.

(29) Shiku, H.; Akeda, T.; Yamada, H.; Matsue, T.; Uchida, I. *Anal. Chem.* **1995**, *67*, 312–317.

(30) Liu, B.; Rotenberg, S. A.; Mirkin, M. V. *Proc. Natl. Acad. Sci. U.S.A.* **2000**, *97*, 9855.

(31) Wang, J.; Polsky, R.; Xu, D. *Langmuir* **2001**, *17*, 5739–5741.

(32) Wang, J.; Xu, D.; Kawde, A.-N.; Polsky, R. *Anal. Chem.* **2001**, *73*, 5576–5581.

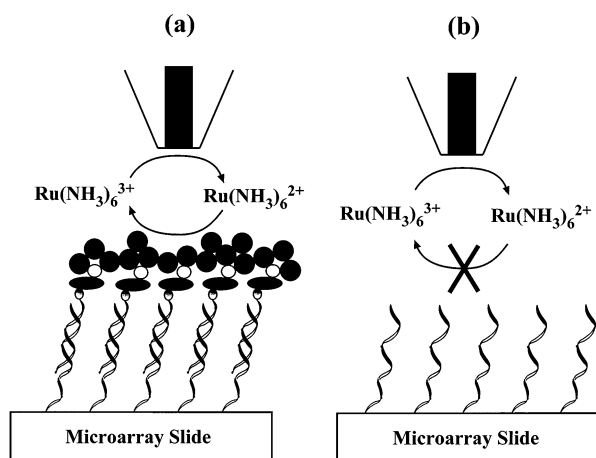


Figure 1. Schematic representation of SECM imaging of DNA hybridization on a microarray. The attachment of the streptavidin–gold nanoparticles and the silver precipitation at a spot where hybridization has occurred results in a SECM positive feedback. The gray circles represent biotin molecules, whereas the ovals and the empty circles are the streptavidin molecules and the gold nanoparticles, respectively. The silver particles deposited onto the streptavidin–gold nanoparticle conjugates are shown by the filled circles.

DNA hybridization reactions were performed by exposing the arrays to 30 μL of a target solution for 3 h. Four different biotinylated target concentrations (0.051, 0.10, 5.1, and 51 nM) were used. While most hybridization reactions were performed at room temperature, the experiments addressing sequence-specific DNA analysis or the differentiation of single-base mismatch were conducted at an elevated temperature. For the 27mer with one single-base mismatch (probe 2), we found that elevating the temperature to 43 $^{\circ}\text{C}$ greatly prohibited the formation of the corresponding duplex. Upon completion of the hybridization reactions, each slide was washed four times with a 10 mM maleate buffer (pH 7.5) containing 15 mM NaCl and 0.1% Tween. To enhance the hybridized spots using the silver staining process, each slide was incubated for 45 min in the streptavidin–gold conjugate solution, followed by washing five times with a buffer solution and incubating in 200 μL of the Silver Blue solution for 10 min at room temperature. Such an incubation time has been shown to result in a large amount of silver deposition at the streptavidin–gold conjugate without a significant nonspecific silver precipitation.¹⁰ We conducted the silver deposition in the dark, and the composition of the Silver Blue solution has been optimized to reduce or eliminate nonspecific silver deposition.¹⁰ Finally, the slide was washed with deionized water and air-dried prior to SECM imaging.

(b) *SECM Imaging of DNA Hybridization at the Microarray Surface.* The developed microarray slide was immersed in a 0.1 M phosphate buffer solution (pH 7.0) containing 2 mM $\text{Ru}(\text{NH}_3)_6^{3+}$. The UME tip was brought to ca. 7 μm above the microarray surface by monitoring the steady-state reduction current of $\text{Ru}(\text{NH}_3)_6^{3+}$ at -0.4 V versus Ag/AgCl. Although our SECM instrument is capable of scanning a 5 cm \times 5 cm area, for illustrative purposes images of smaller areas (e.g., 0.24 cm \times 0.24 cm or 0.18 cm \times 0.18 cm) were shown in this work.

3. Results and Discussion

A schematic diagram of SECM imaging of localized DNA hybridization reactions at a microarray surface is shown in Figure 1. Two scenarios are encountered when SECM is used in conjunction with the silver enhancement. Figure 1a shows the SECM positive feedback behavior when the UME tip is scanned over an area where DNA hybridization has taken place. The formation of the probe–biotinylated target duplex introduces the biotin residue onto the surface, which in a subsequent step will lead to the formation of the biotin/streptavidin–colloidal gold conjugate. As shown in several reports,^{7,10,33} areas covered

with such a conjugate can be further developed through the deposition of silver particles. As a result, this particular spot on the microarray surface becomes conductive and can convert the product diffused from the tip electrode back to the original reactant (in the case shown by Figure 1a, oxidation of $\text{Ru}(\text{NH}_3)_6^{2+}$ back to $\text{Ru}(\text{NH}_3)_6^{3+}$). When the biotinylated target has a sequence noncomplementary to that of the surface-confined DNA probes (Figure 1b), no hybridization will occur, prohibiting the biotin/streptavidin–colloidal gold conjugate and the subsequent silver enhancement from occurring. Consequently, a SECM negative feedback response will be observed. As will be revealed below, the unique capability of SECM for the differentiation of conductive regions from insulating ones facilitates the detection of the DNA hybridization at a level that appears to be as sensitive as fluorescence detection,¹⁰ scanometric DNA array detection with nanoparticle probes,⁷ or colorimetric determination.¹⁰

Before using SECM to scan multiple spots across a given DNA microarray area, we evaluated the analytical performance of SECM for the detection of localized DNA hybridization reactions. First, the sequence specificity of the DNA microarray combined with the biotin/streptavidin–colloidal gold conjugate formation/silver enhancement was examined with SECM. Shown in Figure 2a is a SECM image of an area containing probes 1 (perfectly complementary) and 4 (entirely noncomplementary) that were exposed to a biotinylated target solution and underwent the posthybridization silver staining process. The SECM image indicates that probe 4, whose base sequence is noncomplementary to that of the target, did not result in any appreciable silver particle deposition (no bright spot appears on the left half of Figure 2a). The appearance of the conductive region on the right half of the image, on the other hand, suggests that hybridization had occurred at the spot containing DNA probes that are complementary to the target.

Mirkin and co-workers have demonstrated that interaction of ODN probes with ODN targets labeled with Au nanoparticles substantially alters the melting profiles of the resultant duplex,⁷ allowing single-base mismatch to be determined. While our approach differs from theirs in that the DNA targets are tagged with different molecules (biotin vs gold nanoparticles) and it is not straightforward to compare the sensitivity and detection levels between these two approaches, a useful detection method should allow sequence-specific DNA analysis to be performed at a sensitive level. We found that at room temperature, a spot covered by a probe with three mismatching bases (probe 3) did not produce a SECM positive feedback signal (left half of Figure 2b). This implies that SECM can differentiate the region containing probes with a few mismatching bases from that covered with the complementary probe. However, hybridization of the biotinylated target with a probe containing a single-base mismatch (probe 2) exhibited a circular region with higher tip currents (right side of Figure 2b), indicating that some hybridization had occurred. Our observation of the small extent of hybridization at room temperature is consistent with that from similar studies of heterogeneous DNA sensors using other analytical techniques (e.g., quartz crystal microbalance^{34–38} and surface plasmon reso-

(33) Holgate, C. S.; Jackson, P.; Cowen, P. N.; Bird, C. C. *J. Histochem. Cytochem.* **1983**, *31*, 938–944.

(34) Wang, J.; Palecek, E.; Nielsen, P.; Rivas, G.; Cai, X.; Shiraishi, H.; Dontha, N.; Luo, D.; Farias, P. *J. Am. Chem. Soc.* **1996**, *118*, 7667–7670.

(35) Wang, J.; Nielsen, P. E.; Jiang, M.; Cai, X.; Fernandes, J. R.; Grant, D. H.; Oszoz, M.; Beglieter, A.; Mowart, M. *Anal. Chem.* **1997**, *69*, 5200–5202.

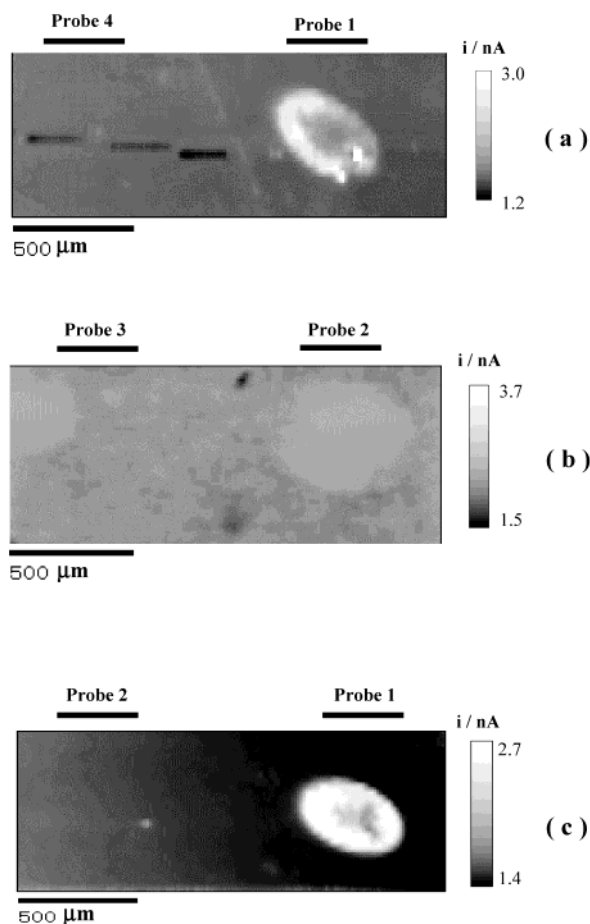


Figure 2. SECM images of spots covered with different probes: (a) a segment of a microarray containing noncomplementary (left) and complementary (right) probes upon hybridization at room temperature, (b) a segment of a microarray covered with probes of three bases (left) and a single base (right) mismatching the sequence of the target upon hybridization at room temperature, and (c) a segment of a microarray containing a probe with a single-base mismatch (left) and a complementary probe (right) upon hybridization at 43 °C. The scale bar has a unit of μm and the current scale is shown in nA. In all of the experiments, $\text{Ru}(\text{NH}_3)_6^{3+}$ (2.0 mM, pH 7.0 phosphate buffer) was used as the SECM mediator and a 5.1 nM target DNA solution was employed for the hybridization.

nance^{39–42}). We further found that elevating the hybridization temperature (43 °C) permitted the discrimination of the probes with a single-base mismatch from that with a complementary sequence (comparing the left and right sides of Figure 2c). This is in reasonable agreement with the report by Caruana and Heller who found that the single-base mismatch of an 18-base ODN immobilized on an enzyme-modified UME could be detected amperometrically at a temperature higher than 45 °C.⁴³ Thus our results suggest that a judicious choice of the hybridization temperature could provide the needed sequence

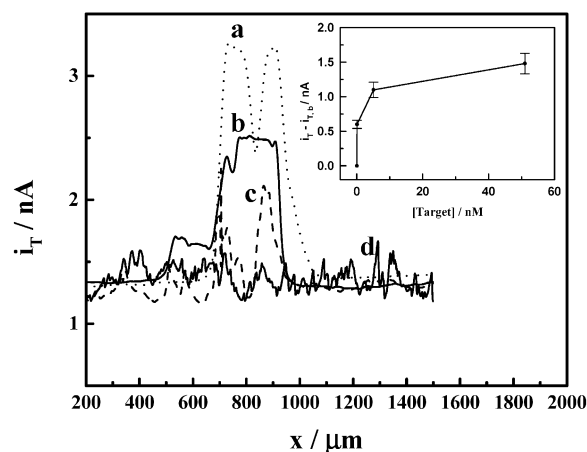


Figure 3. Cross-sectional SECM line scans over spots covered with different amounts of DNA duplexes formed between complementary probe and target molecules. Curves a, b, c, and d correspond to the exposure of probe spots to 51 nM (15 fmol), 5.1 nM (1.5 fmol), 0.1 nM (0.030 fmol), and 0.051 nM (0.015 fmol) targets, respectively. The inset is a plot showing the normalized tip current (average of values over three identical spots) vs concentrations of the biotinylated DNA target.

specificity. This capability is particularly attractive, since analysis of single nucleotide polymorphism (SNP) is useful in disease diagnostics.⁴⁴ It is also interesting to compare the SECM responses to the different extents of hybridization of the same probe at two temperatures. For example, a comparison of the brightness of the spot in Figure 2a with that of the spot in Figure 2c indicates that more targets have formed duplexes with the surface-confined probes when the hybridization reaction was carried out at an elevated temperature.

The effect of target concentration on the extent of hybridization and the detection level of DNA hybridization by SECM was also examined. The SECM line scans over spots covered with different amounts of DNA duplexes (Figure 3) and the relationship between the tip current and the target concentration (i_T –[target], inset) both show that the SECM feedback current increased with the target concentration. It is apparent that the current began to level off as the target concentration approached 5.1 nM (1.5 fmol of total target per spot). This leveling-off suggests that the surface was fully covered by silver particles. Our result is consistent with the 10 nM saturation limit determined by Alexandre et al. using colorimetric detection.¹⁰ The full coverage of silver is also reflected by the plot of the normalized current–distance curve (i.e., SECM approach curve) described below. As the target concentration decreased (e.g., 0.10 nM target concentration or 3.0 fmol of total target), the spot became more difficult to resolve by SECM (curve c in Figure 3). When the target concentration (the total amount of the target) was decreased to 0.051 nM, essentially no spot could be discerned from the rest of the microarray surface (curve d in Figure 3). It should be stated that 0.050 nM corresponds to a total of 1.5 fmol per slide (covering 100 DNA spots) or 0.015 fmol per spot. This observation suggests that the concentration detection level for the formation of this particular duplex is between 0.10 and 0.051 nM. The detection limit of this method, based on the ratio of $3s/m$ (where s is the standard deviation of the blank and m is the slope of the calibration curve), was estimated to be 0.07 nM (or 0.021 fmol per spot on the

(36) Cavic, B. A.; Hayward, G. L.; Thompson, M. *Analyst* **1999**, *124*, 1405–1420.

(37) Thompson, M.; Furtado, L. M. *Analyst* **1999**, *124*, 1133–1136.

(38) Okahata, Y.; Kawase, M.; Niikura, K.; Ohtake, F.; Furusawa, H.; Ebara, Y. *Anal. Chem.* **1998**, *70*, 1288–1296.

(39) Silin, V.; Plant, A. *Trends Biotechnol.* **1997**, *15*, 353–359.

(40) Gotoh, M.; Hasecawa, Y.; Shinohara, Y.; Shimizu, M.; Tosu, M. *DNA Res.* **1995**, *2*, 285–293.

(41) Peterlinz, K. A.; Georgiadis, R. M.; Herne, T. M.; Tarlov, M. J. *J. Am. Chem. Soc.* **1997**, *119*, 3401–3402.

(42) Nelson, B. P.; Grimsrud, T. E.; Liles, M. R.; Goodman, R. M.; Corn, R. M. *Anal. Chem.* **2001**, *73*, 1–7.

(43) Caruana, D. J.; Heller, A. *J. Am. Chem. Soc.* **1999**, *127*, 769–774.

(44) Watson, J.; Gilman, M.; Witkowski, J.; Zoller, M. *Recombinant DNA*, 2nd ed.; W. H. Freeman: New York, 1992.

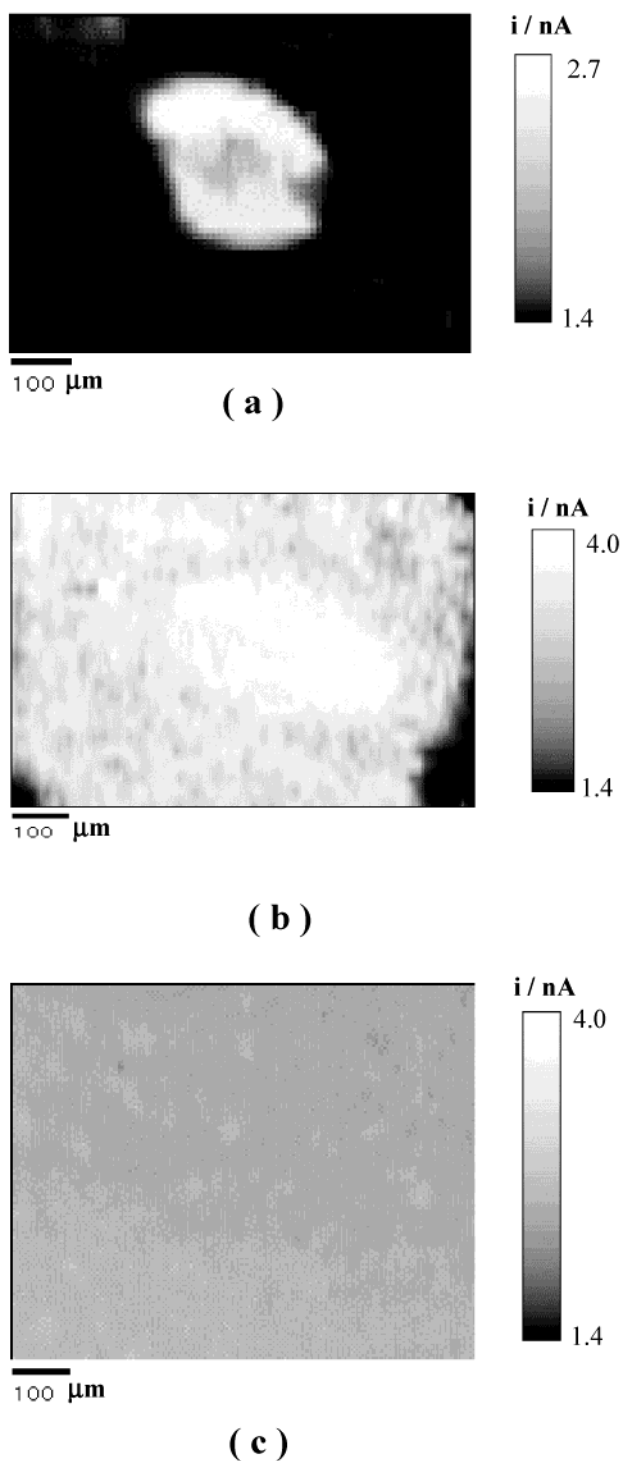


Figure 4. SECM images of spots covered with a probe upon hybridization with different amounts of its complementary target: (a) 1.5 fmol, (b) 0.030 fmol, and (c) 0.015 fmol at each spot. The hybridization reactions were carried out at 43 °C.

slide). The absolute target quantity resulting in the development (appearance) of the spot in Figure 3c was 0.030 fmol. Fluorescence and colorimetric detections for a polynucleotide target were both at 0.1 fmol.¹⁰ While these detection levels are not directly comparable because of the differences in the target sizes and the surface densities of the duplexes, the detection level or limit of our approach is low and in the range of (if not lower than) that of other methods. Similarly, it is difficult to compare the detection level of the scanometric DNA detection⁷ to that of the present method, because gold nanoparticles, instead of

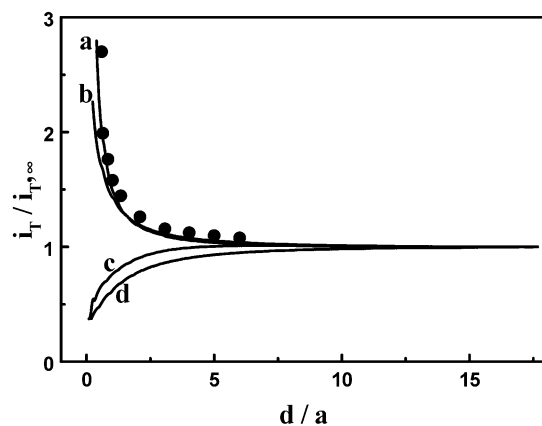


Figure 5. Normalized current–distance curves recorded over spots covered with different amounts of silver particles: 1.5 fmol (curve a), 0.030 fmol (curve b), and 0.015 fmol (curve c) at each spot. The SECM current–distance behavior over a bare glass surface is shown by curve d, and the theoretical tip current values over a conductive surface are given by the filled circles.

biotin molecules, were directly attached to the DNA targets. Consequently, the surface density of gold nanoparticles, which affect the hybridization efficiency⁴⁵ and the follow-up silver staining process, might be quite different than that at the surface produced with the present method.

Shown in Figure 4a–c are three representative SECM images acquired at portions of three different microarrays that had been subject to the target solutions (5.1, 0.1, and 0.051 nM). These images correlate very well with the line scans shown in Figure 3 in terms of the i_T –[target] relationship.

We attribute the low detection level of SECM for the DNA hybridization at a microarray surface to the remarkable sensitivity of SECM to small variations of surface conductivities caused by the follow-up silver particle deposition. Figure 5 shows a series of current–distance curves (i_T – d , SECM approach curves) over spots covered with different amounts of duplexes. When the target concentration was high (curve a), the approach curve becomes congruent with the theoretical values over a conductive substrate. This suggests that the surface had been fully covered with silver particles. Thus, SECM will not detect amounts greater than this level (5.1 nM or 1.5 fmol of target per spot), because the deposition of more silver particles will not further increase the SECM current. On the other hand, lower target levels will drastically alter the SECM approach curves (curves b and c) from the behavior over conductive substrates to that over surfaces with finite heterogeneous electron-transfer kinetics⁴⁶ (i.e., behaviors between completely conductive and insulating situations).

Finally, we demonstrate that SECM is suitable for imaging a relatively large area on a microarray surface. Figure 6 is a SECM image displaying a section of a microarray (0.24 cm × 0.24 cm) containing six discrete spots onto which probe 1 had been immobilized. Relatively regular and well-separated spots can be visualized. These spots, with a separation of about 500–750 μm (center to center), have an average diameter of ca. 400–500 μm. The brightness (i.e., the magnitude of the SECM feedback current) is relatively even, suggesting that hybridization

(45) Demers, L. M.; Mirkin, C. A.; Mucic, R. C.; Reynolds, R. A., III; Letsinger, R. L.; Elghanian, R.; Viswanadham, G. *Anal. Chem.* **2000**, *72*, 5535–5541.

(46) Bard, A. J.; Mirkin, M. V.; Unwin, P. R.; Wipf, D. O. *J. Phys. Chem.* **1992**, *96*, 1861–1868.

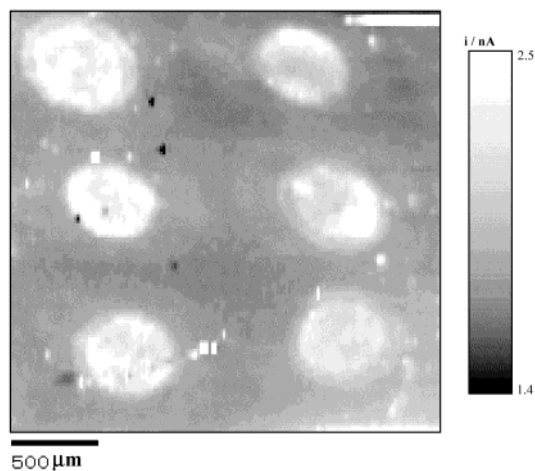


Figure 6. A SECM image of six spots of the same probe on a microarray surface. The hybridization of the probe with its complementary target (51 nM) was conducted at room temperature.

of the target happened at all of the spots covered by the same DNA probe. The DNA microarray using our homemade spotting device is of low density² (about 100 spots/cm²), due to the imperfection of the homemade spotting device and the inconsistency in the manual translation of the glass slide between consecutive DNA spotting processes. Given the theoretical prediction that positive feedback can be observed at a spot whose diameter is only 4 times as large as that of the UME tip (i.e., at a spot slightly greater than 44 μm in diameter for a 11- μm -diameter UME tip),⁴⁶ it should be feasible to image microarrays of a much higher density with the SECM. If the spot-to-spot separation and the spot size can both be reduced by 10-fold, we predict that a microarray with a density of 100 000 spots/slide can be mapped out by SECM under the same experimental conditions. Such a density corresponds to the higher limit of the medium-density DNA microarray and would make SECM an attractive technique for biochip imaging. SECM imaging of an area of 0.24 cm \times 0.24 cm can be completed in about 38 min at a tip scanning speed of 50 $\mu\text{m/s}$. Although a typical commercial fluorescence scanner can image a slide of similar dimensions in as little as 10–15 min, the SECM approach is less expensive and more substrate-general (e.g., microarrays based on nylon or other less reflective materials). The throughput is satisfactory for most ap-

plications involving gene expression and sequence analysis,² making SECM an imager complementary to commercial fluorescence scanners in selected applications.

4. Conclusion

Imaging of localized DNA hybridization at a DNA microarray by SECM has been demonstrated. The method relies on the inherent sensitivity of SECM to the detection of the small variation of the surface conductivities. Utilizing the streptavidin–gold nanoparticle attachment and the silver precipitation at a spot possessing the complementary probe, the formation of the probe–biotinylated target duplex significantly amplified the SECM tip current. Coupled with the alteration of the hybridization temperature, highly sequence-specific (single-base mismatch) DNA analysis can be accomplished. The method was also found to yield a low detection level. A 17mer target of a quantity as low as 30 amol per spot can be determined. While the detection level is not directly comparable to those for polynucleotides using fluorescence (0.1 fmol) and colorimetric detections (0.1 fmol), the detection level of the SECM method is also low and should be sufficient for most applications involving gene expression and sequence analysis. Moreover, the SECM detection is relatively inexpensive and is substrate (microarray materials)-general. Although the concept of using SECM to image DNA microarrays is demonstrated only with a low-density chip fabricated in house, the SECM theory predicts that visualization of a medium-density DNA array should be highly possible. Compared to other types of scanning probe microscopy (e.g., scanning tunneling microscopy and atomic force microscopy), the SECM should be the method of choice for the purpose of reading a microarray, due to the compatibility of its scanning parameters (e.g., the scanning speed and area scanned) to the microarray dimensions (total chip area and the spot size).

Acknowledgment. Partial support of this work by a NIH-SCORE Subproject (GM08101), a NIH-AREA Grant (GM 63530-01), and a NSF-CRUI Grant (DBI-9978806) is gratefully acknowledged. We also thank Dr. D. Wipf (Mississippi State University) for providing us with the updated SECM software and Mr. D. Ralin (Maven Technologies, LLC) for his help and constructive discussions.

LA011822S